

**Towards organic carbon isotope records from stalagmites: coupled  $\delta^{13}\text{C}$  and  $^{14}\text{C}$  analysis using wet chemical oxidation**

Franziska A. Lechleitner<sup>1,2,3\*</sup>, Susan Q. Lang<sup>4</sup>, Negar Haghipour<sup>2,5</sup>, Cameron McIntyre<sup>6</sup>, James U.L. Baldini<sup>3</sup>, Keith Prufer<sup>7</sup>, Timothy I. Eglinton<sup>2</sup>

<sup>1</sup>Department of Earth Sciences, University of Oxford, South Parks Road, Oxford OX1 3AN, UK

<sup>2</sup>Department of Earth Sciences, ETH Zurich, Sonneggstrasse 5, 8092 Zurich, Switzerland

<sup>3</sup>Department of Earth Sciences, University of Durham, Science Site, Durham DH1 3LE, UK

<sup>4</sup>School of the Earth, Ocean, and Environment, University of South Carolina, 701 Sumter Street, EWS 617, Columbia SC 29208, USA

<sup>5</sup>Laboratory of Ion Beam Physics, Department of Physics, ETH Zurich, Otto-Stern-Weg 5, 8093 Zurich, Switzerland

<sup>6</sup>Scottish Universities Environmental Research Centre (SUERC), Rankine Avenue, East Kilbride G75 0GF, UK

<sup>7</sup>Department of Anthropology, University of New Mexico, Albuquerque, NM 87106, USA

Keywords: organic matter, stalagmite, carbon isotopes, bomb spike

\*corresponding author: [franziska.lechleitner@earth.ox.ac.uk](mailto:franziska.lechleitner@earth.ox.ac.uk)

**ABSTRACT**

Speleothem organic matter can be a powerful tracer for past environmental conditions and karst processes. Carbon isotope measurements ( $\delta^{13}\text{C}$  and  $^{14}\text{C}$ ) in particular can provide crucial information on the provenance and age of speleothem organic matter, but are challenging due to low concentrations of organic matter in stalagmites. Here, we present a method development study on extraction and isotopic characterization of speleothem organic matter using a rapid procedure with low laboratory contamination risk. An extensive blank assessment allowed us to quantify possible sources of contamination through the entire method. Although blank contamination is consistently low ( $1.7 \pm 0.34 - 4.3 \pm 0.86 \mu\text{g C}$  for the entire procedure), incomplete sample decarbonation poses a still unresolved problem of the method, but can be detected when considering both  $\delta^{13}\text{C}$  and  $^{14}\text{C}$  values. We test the method on five stalagmites, showing reproducible results on samples as small as  $7 \mu\text{g C}$  for  $\delta^{13}\text{C}$  and  $20 \mu\text{g C}$  for  $^{14}\text{C}$ . Furthermore, we find consistently lower non-purgeable organic carbon (NPOC)  $^{14}\text{C}$  values compared to the carbonate  $^{14}\text{C}$  over the bomb spike interval in two stalagmites from Yok Balum Cave, Belize, suggesting overprint of a pre-aged or even fossil source of carbon on the organic fraction incorporated by the stalagmites.

**Commented [SSE1]:** I think that this is a really fundamental observation

## INTRODUCTION

Organic matter entrapped in speleothem carbonate is increasingly recognized as a promising tool for the reconstruction of past ecosystem and climate change (Blyth et al., 2016; Bosle et al., 2014; Heidke et al., 2018; Perrette et al., 2015; Quiers et al., 2015). Organic carbon (OC) primarily originates from the overlying soil and karst system from which it is transported into caves by vadose water, or from microbial production within the cave (Blyth et al., 2016). Other sources of OC in cave systems include airborne material, generally limited to areas near the cave entrances, and compounds derived from cave-dwelling animals and insects, which can constitute a major source of OC if large animal populations are present (Blyth et al., 2008). The portion of OC stemming from the surface is argued to be dominant in most karst systems (Baker and Genty, 1999; Perrette et al., 2015; Quiers et al., 2015; Shabarova et al., 2014), but substantial reworking of OC is generally observed (Birdwell and Engel, 2010; Einsiedl et al., 2007; Lechleitner et al., 2017; Shabarova et al., 2014). Nevertheless, OC incorporated in stalagmites is considered a potentially very sensitive proxy for surface environmental conditions (Blyth et al., 2016, 2008).

Isotopic studies on carbon can provide insight into provenance, processing, and age of organic matter in environmental matrices. Stable carbon isotope ratios ( $\delta^{13}\text{C}$ ) in biogenic samples are generally strongly fractionated by metabolic processes. Higher plants utilizing the C3 carbon fixation pathway exhibit very negative  $\delta^{13}\text{C}$  values (-32 to -22‰), whereas C4 plants fractionate less strongly (-16 to -10‰) (Vogel, 1980). Radiocarbon ( $^{14}\text{C}$ ), in contrast, provides a measure of the age of OC analysed, indicating its recalcitrance and turnover time.

The conventional understanding is that OC incorporated in stalagmites is not directly affected by the addition of  $^{14}\text{C}$ -dead carbon from limestone dissolution (Blyth et al., 2017), and may thus provide important constraints on drivers of the karst carbon cycle, and on (past) surface conditions.

Because of the very low amounts of organic carbon found in stalagmites embedded in a matrix virtually exclusively derived of carbonate, large sample sizes typically need to be processed for analysis and careful treatments are needed to remove inorganic carbon and other interferences. Both increase the potential for contamination through laboratory procedures, rendering such measurements challenging (Wynn and Brocks, 2014). Moreover, the effect of large sample sizes on their chronological assessment needs to be considered, e.g., through sampling along growth layers where possible (fast growing stalagmites). Thus far, a few studies on  $\delta^{13}\text{C}$  in non-purgeable organic carbon (NPOC) incorporated in stalagmites have been conducted (Blyth et al., 2013b, 2013a) using an approach based on acid digestion of stalagmite samples to remove inorganic carbon from  $\text{CaCO}_3$ , followed by oxidation of the carbon remaining in the solution to  $\text{CO}_2$ , from which  $\delta^{13}\text{C}$  can then be determined. Their results show that accurate and reproducible  $\delta^{13}\text{C}$  measurements are possible from stalagmites, using relatively small sample

amounts (100-200 mg CaCO<sub>3</sub>). To our knowledge, the only published studies on stalagmite OC <sup>14</sup>C to date concentrate on the use of speleothems with high OC concentrations for dating purposes (e.g., Blyth et al., 2017; Borsato et al., 2000; Genty et al., 2011). Thus far, however, there have been no reported <sup>14</sup>C measurements on stalagmite NPOC, likely because sample size requirements are substantially greater, with attendant increases in procedural blanks and other analytical uncertainties. The latter limitation is partly alleviated by recent developments in accelerator mass spectrometry that permit analysis of small (<20 µg C) samples (Fahrni et al., 2013; Ruff et al., 2007). Here, we describe a suite of experiments conducted to develop an extraction and oxidation procedure that builds on prior developments (Lang et al., 2016, 2013, 2012), and show results from its application for studies of both δ<sup>13</sup>C and <sup>14</sup>C of NPOC preserved in stalagmites. After testing the method on three stalagmite samples, we applied it on two well-dated stalagmites from Yok Balum Cave, Belize (YOK-G and YOK-I). Both stalagmites were previously sampled for high-resolution inorganic <sup>14</sup>C (Lechleitner et al., 2016a; Ridley et al., 2015), revealing a very clear imprint of bomb <sup>14</sup>C in the carbonate phase. Because of high growth rates in these stalagmites, enough sample material was available to analyse NPOC <sup>14</sup>C before and after the bomb pulse, providing an opportunity to study the organic carbon cycle in cave systems from a <sup>14</sup>C perspective for the first time.

## MATERIALS

### Stalagmite Samples

Five different stalagmites of different provenance, age, and mineralogy were used for this preliminary study (Table 1, Fig. 1). Stalagmites are prone to OC contamination, either from improper handling or outside influences (Wynn and Brocks, 2014). Therefore, any method attempting to extract a primary NPOC signal from these samples needs to consider and eliminate the possibility of sample contamination, particularly on the stalagmite surface. In this study, two methods for the removal of contaminated surfaces were applied. The test stalagmites TSAL, BB2, and YOK-K were available as discrete sample pieces. In this case, the entire sample was leached with 1N HCl to remove about 1g of CaCO<sub>3</sub> (5-20% of total mass) from all surfaces. After leaching, the samples were washed three times with ultrapure water and dried in an oven at 60°C, before being powdered to homogeneity using an agate mortar pre-cleaned with methanol and dichloromethane. All sample powders were stored in pre-combusted glass vials with acid-washed Teflon caps (storage time varied from days to months, depending on the sample).

For stalagmites YOK-I and YOK-G, smaller samples were drilled from specific depths to capture the bomb spike interval. For YOK-I, this was achieved by drilling samples using a hand-held drill (Dremel 4000) equipped with newly purchased diamond-coated drill bits. The drill bits were pre-cleaned by extracting them three times using methanol, dichloromethane,

**Commented [SSE2]:** Could we elaborate a bit here?  
Listing at least the cave here would be useful

and ultrapure water, and dried in an oven at 60°C overnight. Before drilling, dust and particles were removed from the stalagmite surface using compressed air, and the top ~ 1mm was removed using a separate drill bit and discarded. For YOK-G, a new Kodiak carbide end mill was used on a Sureline micromill, and the drill bit was cleaned with HPLC-grade methanol and ultrapure water before and in between sampling. Dust and powder was removed from the stalagmite surface before and between sampling, and the powdered samples from YOK-G were shipped to the laboratory at ETH Zurich in sterile microcentrifuge vials.

Sample ID	Cave	Region	Sampled age	Mineralogy	Colour	Notes
TSAL	Tskaltubo	Caucasus	40 kyr BP	calcite	clear white	
BB2	Blessberg	Germany	6 kyr BP	calcite	brownish	
YOK-K	Yok Balum	Central America	n.d.	aragonite	brown and grey layers	
YOK-I			1910-1980 CE	aragonite	white with grey layers	sampling over bomb spike interval
YOK-G			1940-1980 CE	aragonite	clear white	

**Table 1.:** Details of the stalagmites used. Sample ages are given in kyr BP (thousands of years before present, with the present defined as 1950 CE), or as CE, i.e., Common Era.

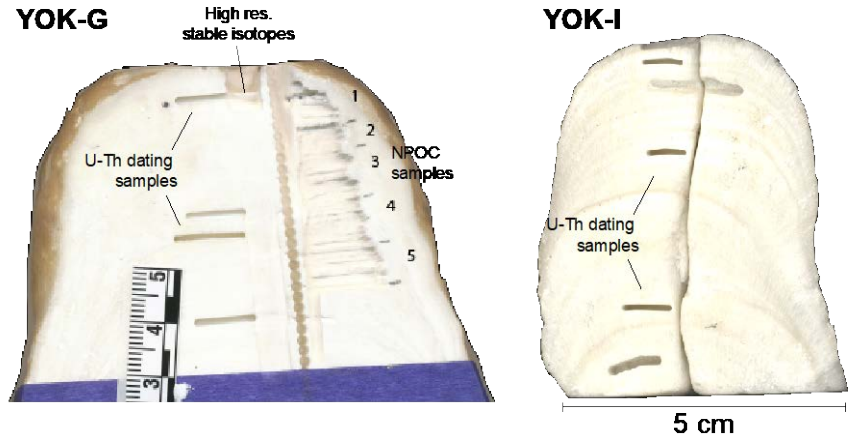


**Fig. 1.:** Top sections of stalagmites YOK-G and YOK-I from Yok Balum Cave, Belize. In this study, the bomb spike interval was targeted for isotopic characterization of the organic matter entrapped in stalagmite carbonate. For sample YOK-G, the tracks left by drilling for NPOC analysis are visible.

## METHODS

### Decarbonation

Aliquots of the powdered stalagmites were transferred to pre-combusted 12 ml borosilicate Exetainer screw-capped vials with butyl rubber septa (Labco, High Wycombe, UK). Decarbonation of the samples to remove inorganic carbonate proceeded by adding 1.5 ml of 85%  $\text{H}_3\text{PO}_4$  (puriss. grade), followed by 3.5 ml of ultrapure water ( $18.2 \text{ M}\Omega$  and  $\leq 5 \text{ ppb TOC}$ ) (Fig. 2). Acid and water were added stepwise and the vials were briefly vortexed in between to ensure complete submersion of the  $\text{CaCO}_3$ . The samples were then left to dissolve on the laboratory bench (room temperature:  $23^\circ\text{C}$ ) covered with clean aluminium foil or acid-washed vial caps. Because traditional  $\text{CaCO}_3$  dissolution protocols (i.e., purging the solution with He for 5-10 min) resulted in residual inorganic carbon contributions in the final extracts (as indicated by high  $\delta^{13}\text{C}$  values,  $\sim -9\text{‰}$ ), we tested several approaches to ensure complete decarbonation of the samples. Early attempts involved subjecting the samples to gentle vacuum using a rotary evaporator, as successfully demonstrated by Blyth et al. (2013a), but this was quickly abandoned due to substantial blank contributions encountered with this method in our laboratory (Suppl. fig. 1). More efficient and less detrimental methods in terms of blank contributions were (i) to place the samples in a desiccator that was evacuated using a hand-held pump for a few days while periodically renewing the vacuum, or (ii) to subject the closed sample vials to sonication by placing them in an ultrasonic bath at room temperature for 30-45 min during acidification.

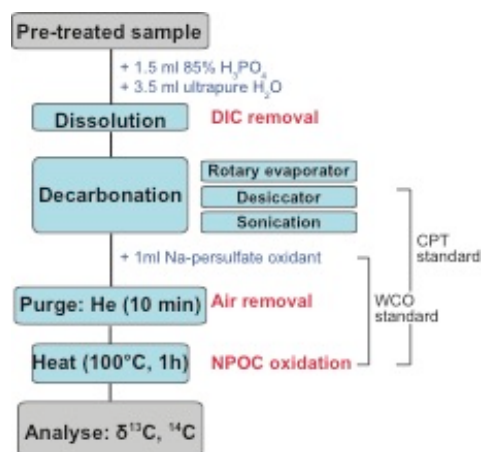


**Fig. 2.:** Flowchart describing the method. The method steps covered by WCO and chemical pre-treatment (CPT) standards for blank assessment are indicated.

### Wet Chemical Oxidation and Isotope Analysis

After decarbonation, organic carbon was converted to  $\text{CO}_2$  using a wet chemical oxidation (WCO) approach (described in Lang et al., 2016, 2013, 2012, Fig. 2). Briefly, sodium persulfate

(Sigma, purum p.a.  $\geq 99.0\%$ , further purified by recrystallization) was added as an oxidant (1 ml; solution: 1.5g  $\text{Na}_2\text{S}_2\text{O}_8$  in 50 ml ultrapure water) after the decarbonation. All vials were capped and purged for  $\sim 10$  min using ultrapure helium to remove ambient air and remaining inorganic  $\text{CO}_2$  in the vials. For the oxidation to take place, the vials were then heated to  $\sim 100^\circ\text{C}$  for one hour (Fig. 2). The headspace  $\text{CO}_2$  resulting from oxidation of the NPOC was analysed for  $\delta^{13}\text{C}$  on a Thermo Delta V Plus isotope ratio mass spectrometer (IRMS) coupled with a ThermoFinnigan GasBench II carbonate preparation device at the Geological Institute, ETH Zurich, following the method described in Lang et al. (2012).  $\delta^{13}\text{C}$  values are reported as  $^{13}\text{C}/^{12}\text{C}$  ratios expressed as the permil deviation from the international Vienna Pee Dee Belemnite standard (VPDB).  $^{14}\text{C}$  measurements were performed as described in Lang et al. (2016) using a MICADAS AMS equipped with a Gas Ion Source (GIS) at the Laboratory for Ion Beam Physics (LIP) at ETH Zurich. AMS background correction and data normalization were carried out using the software BATS (Wacker et al., 2010) and  $^{14}\text{C}/^{12}\text{C}$  ratios are reported as  $F^{14}\text{C}$  according to (Reimer et al., 2004).

#### Blank Assessment

Sucrose (Sigma,  $\delta^{13}\text{C} = -12.4\text{‰}$  VPDB,  $F^{14}\text{C} = 1.053 \pm 0.003$ ) and phthalic acid (Sigma,  $\delta^{13}\text{C} = -33.6\text{‰}$  VPDB,  $F^{14}\text{C} < 0.0025$ ) were used as standards to evaluate blank contributions from the different steps of the method. These standards were chosen for their distinct isotope signatures, which allow to capture different contamination end members, and their solubility in water (Lang et al., 2016).

The contribution of extraneous carbon to the WCO was evaluated by a suite of standards (*WCO standards*) prepared for each run by adding varying amounts of standard solution to vials containing 5 ml of ultrapure water, then taking them through the WCO procedure. To evaluate the mass and  $F^{14}\text{C}$  of extraneous carbon for each run, we used the model of constant contamination described in Hanke et al. (2017) and Haghipour et al. (2018). The procedural blank of the decarbonation (*chemical pre-treatment standard*) was quantified by spiking vials containing acid with variable amounts of sucrose and phthalic acid, before taking them through the entire procedure (Fig. 2). The decarbonation efficiency and possible carbonate matrix effects were tested by analysing carbonate samples with no oxidant added, and/or by spiking IAEA-C1 (carbonate  $F^{14}\text{C} = 0$ , NPOC presumed  $^{14}\text{C}$ -dead) samples with known amounts of standard solution. Finally, we tested whether contamination from the rubber septa might pose an issue with prolonged storage times of prepared extracts (three weeks). This was achieved by preparing chemical pre-treatment standards that were subsequently measured in two batches, the first one day and the second three weeks after preparation.

## RESULTS

## Blank Assessment

Because of the typically low amount of extraneous carbon in WCO samples, standard curves were used to assess blank contamination in each run. Using two standards with very different  $F^{14}C$  and  $\delta^{13}C$  values allows quantification of the amount and isotopic composition of the blank (Hanke et al., 2017; Lang et al., 2016). All runs were corrected for extraneous carbon contributions following the methodology by Hanke et al. (2017) for  $F^{14}C$  and Lang et al. (2012) for  $\delta^{13}C$  (not discussed here). Both methods assume constant contamination from each method step on all samples.

## Long-Term $^{14}C$ Blank Assessment of WCO Procedure

For the WCO standards (Fig. 3, Table 2), the average blank contamination over all runs was  $1.30 \pm 0.52 \mu g C$ ,  $F^{14}C = 0.42 \pm 0.17$ , when calculated with the method of constant contamination by Haghypour et al. (2018; Suppl. Table 1). However, the fluctuation in the contribution of extraneous carbon varied greatly between runs over the course of the study (2015 – 2018). Within a single run, contamination can be as low as  $0.4 \pm 0.1 \mu g C$  ( $F^{14}C = 0.15 \pm 0.04$ , run C170918NHG1). For six out of the nine runs, contamination remained below  $1.15 \mu g C$  and only two runs had contamination  $> 3 \mu g C$  (Table 2).

Run number	WCO standards				Chemical pre-treatment standards				% blank from WCO
	$F^{14}C_c$	$\sigma_{F^{14}C_c}$ (abs)	mc ( $\mu g$ )	$\sigma_{mc}$ (abs)	$F^{14}C_c$	$\sigma_{F^{14}C_c}$ (abs)	mc ( $\mu g$ )	$\sigma_{mc}$ (abs)	
C180108NHG1	0.21	0.04	1.1	0.2	0.17	0.03	1.7	0.3	65
C170918NHG1	0.15	0.10	0.4	0.1	0.40	0.08	2.5	0.5	32
C160913FLG1	0.32	0.06	1.1	0.2	0.25	0.05	4.0	0.8	27
C160825BLVG1	0.47	0.09	0.9	0.2	0.30	0.06	4.3	0.9	22
C160510TVG1	0.17	0.03	1.8	0.4					
C160224FLG1	0.26	0.05	1.1	0.2					
C150903FLG1	0.11	0.02	3.1	0.6					
C150928FLG1	0.39	0.08	1.1	0.2					
C150602FLG1	0.09	0.02	3.3	0.7					

**Table 2.:** Blank contamination for all AMS runs for WCO standards, as well as the chemical pre-treatment standards (where available).

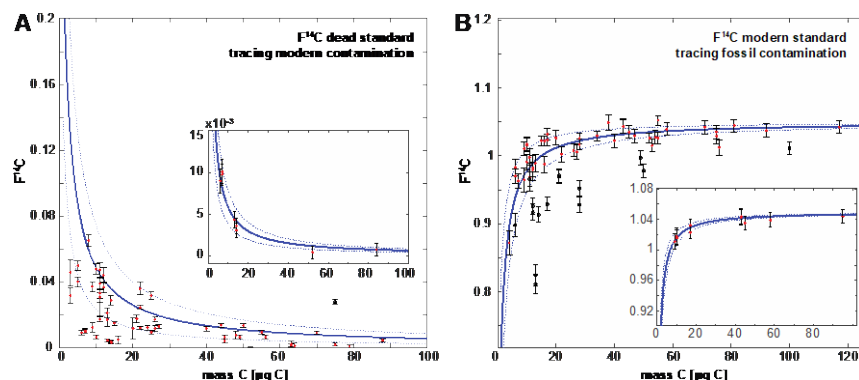


**Fig. 3:** Summary of all WCO standards analysed in the course of the study. A –  $F^{14}C$  of the dead standard, phthalic acid. B –  $F^{14}C$  of the modern standard, sucrose. Outliers are marked in black and were not included in the calculation of the blank contribution. Inserts show values for a single measurement run. The solid blue lines represent the best fit with  $1\sigma$  error ranges. All data is provided in Suppl. Table 1.

### Chemical Pre-Treatment Blank

Overall, the chemical pre-treatment standards show larger blank contamination than the WCO ( $1.7 \pm 0.34 - 4.3 \pm 0.86$  µg C, Table 2, Fig. 4), with the WCO contributing between 22 and 65% (average 37%,  $n=4$ ) of the total extraneous carbon in the samples. The  $F^{14}C$  values between individual chemical pre-treatment and WCO standards were usually within the  $2\sigma$ -bound of each other, although contamination  $F^{14}C$  values were always lower for the chemical pre-treatment standards. Incomplete removal of inorganic  $CO_2$  from the sample solution proved to be one of the main challenges faced during method development. Tests on samples that were not oxidised and processed using the desiccator revealed that 23 out of 42 test vials contained small amounts of residual inorganic carbonate, with enriched  $\delta^{13}C_{CO_2}$  values (average over all samples  $-8.92\text{‰}$  VPDB). Sonication at room temperature also typically resulted in small ( $\sim 0.7$ – $1.5$  µg C) amounts of carbonate left in the solution. Vials containing known amounts of  $^{14}C$ -dead IAEA-C1 carbonate and spiked with phthalic acid show a weak correlation between the amount of carbonate added and the isotopic composition of the WCO extract (Suppl. fig. 2), suggesting a possible influence of sample size on decarbonation efficiency. Rubber septa contamination during extract storage does not appear to be an issue over the timescale investigated here (up to three weeks). We find no significant difference between the average value of sucrose and phthalic acid samples measured before and after storage (sucrose values are within  $1\sigma$  of each other, phthalic acid within  $2\sigma$ , after blank correction).



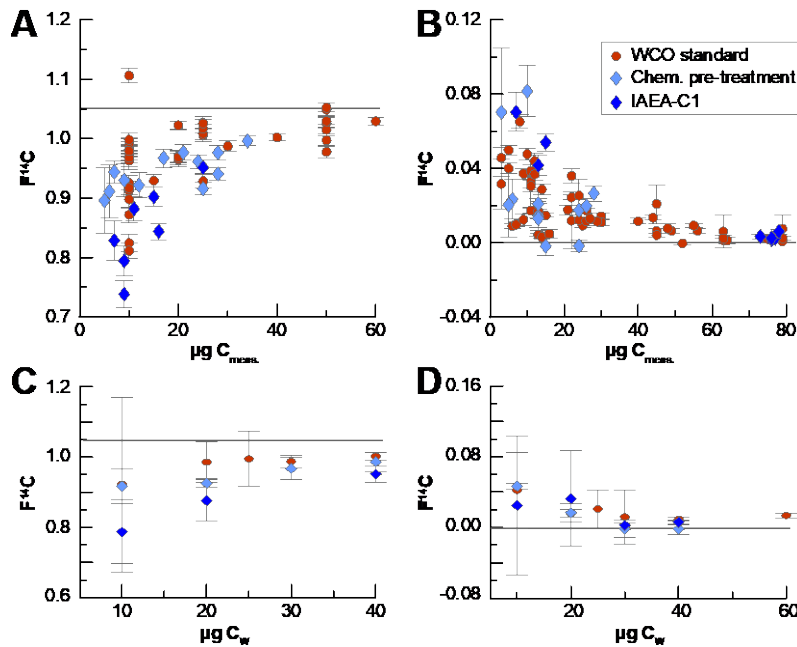


**Fig. 4.:** Comparison between chemical pre-treatment and WCO standards, as well as IAEA-C1-spiked procedural standards, presumed NPOC-dead. A and B - standard curves for sucrose and phthalic acid, respectively, C and D – average of the standard groups per weight class (grouped by amount of standard weighed in).

### Stalagmites

For each stalagmite, the amount of C measured is positively correlated to the initial carbonate sample size, and is fairly reproducible for different initial weights (Fig. 5A, Suppl. Table 2). NPOC concentrations vary greatly between stalagmites, ranging between 0.003 and 0.017 wt% (averages calculated for all samples of one stalagmite), with TSAL yielding the lowest concentrations and YOK-G and YOK-K the highest. These NPOC concentrations are within the range of previously published values for speleothems (0.01 – 0.3 wt%, Blyth et al., 2016; Li et al., 2014; Quiers et al., 2015). Most stalagmite WCO extracts are depleted in  $^{13}\text{C}$ , with  $\delta^{13}\text{C}$  values clustering around -24 – -26‰ VPDB, values typical of C3 vegetation (Fig. 7B). No clear trend in  $\delta^{13}\text{C}$  values between the different stalagmites can be discerned, and the intra-sample variability in  $\delta^{13}\text{C}$  is generally larger than the difference between samples.  $F^{14}\text{C}$  values show no trend with sample size, and appear to be relatively consistent for the different stalagmites (Fig. 5C, Suppl. Table 2). TSAL, the oldest stalagmite (40 kyr) also exhibits the lowest NPOC  $^{14}\text{C}$  activities (average  $F^{14}\text{C} = 0.29$ ), but these values are still significantly higher than the corresponding carbonate value ( $F^{14}\text{C} \sim 0$ , Fig. 5D). Stalagmite

YOK-K (estimated age ~2 kyr) shows the same trend (NPOC  $F^{14}C = 0.52$ ,  $CaCO_3 F^{14}C = 0.24$ ), whereas no difference is found between NPOC and  $CaCO_3$  in stalagmite BB2 (assumed age: 3-6 kyr, NPOC  $F^{14}C = 0.35$ ,  $CaCO_3 F^{14}C = 0.31$ ). For YOK-I and YOK-G (covering the bomb spike interval), the trend is reversed, with the  $CaCO_3 F^{14}C$  higher than the NPOC  $F^{14}C$  (YOK-I: NPOC  $F^{14}C = 0.77$ ,  $CaCO_3 F^{14}C = 1.0$ ; YOK-G: NPOC  $F^{14}C = 0.88$ ,  $CaCO_3 F^{14}C = 1.01$ ).

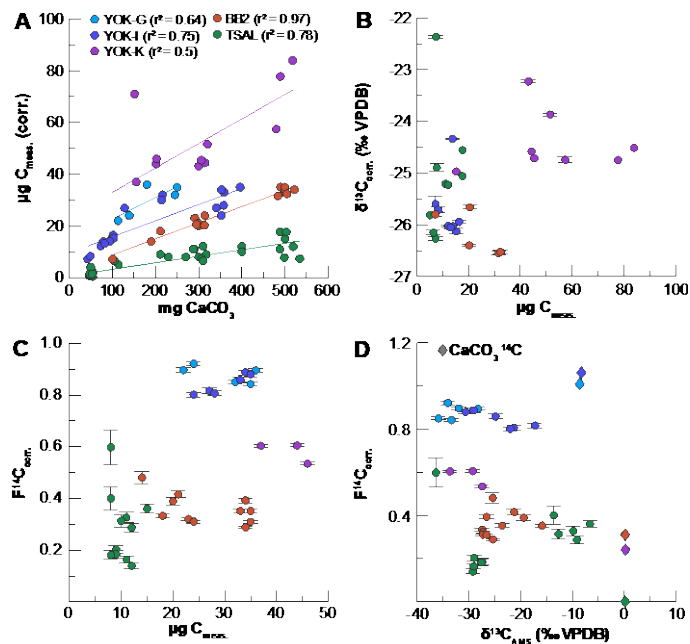


**Fig. 5.:** Results of the stalagmite samples. A – Amount of carbon ( $\mu g C$ ) measured and corrected for procedural blanks vs. weight of  $CaCO_3$  (in  $mg$ ) added to the vials for all stalagmites used in this study. Data is combined from all runs for  $\delta^{13}C$  and  $^{14}C$ . B – Blank corrected  $\delta^{13}C$  values from IRMS vs. amount of C measured. C –  $F^{14}C$  vs. amount of C measured. D –  $F^{14}C$  vs.  $\delta^{13}C$  from the same AMS run. Note that the precision on AMS  $\delta^{13}C$  is  $\pm 2\text{‰}$ . Diamonds denote the corresponding values measured on carbonate samples.

The pre- and post-bomb spike NPOC samples from stalagmites YOK-I and YOK-G both show an increase in  $F^{14}C$  with the bomb spike (Fig. 6). However, in both cases, the NPOC  $F^{14}C$  is lower than the contemporaneous carbonate  $F^{14}C$ . Samples from the first batch of samples from YOK-I (YOK-I A, analysed in May 2016) have markedly lower  $F^{14}C$  and less negative  $\delta^{13}C$  values compared to both a previous analysis and to the samples of YOK-G (Suppl. Fig. 4).

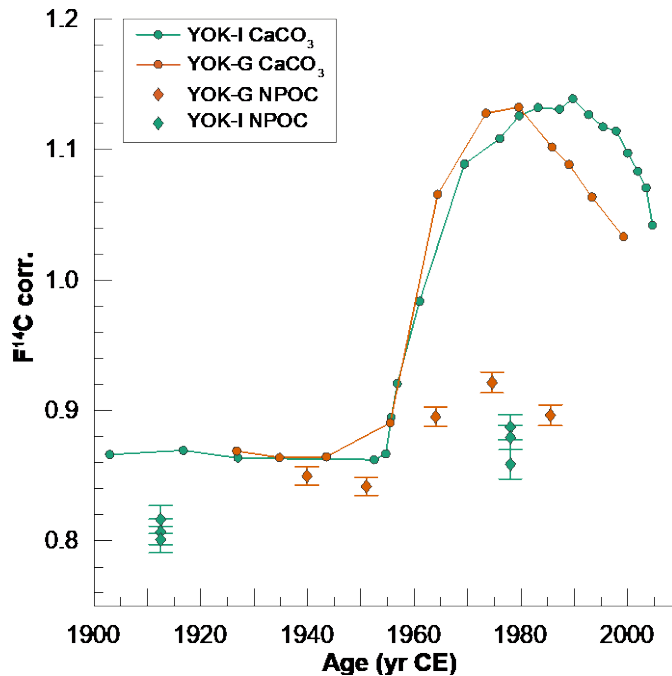


**Fig. 6.:** Comparison between the bomb spike measured in stalagmites YOK-I and YOK-G carbonate with the results from WCO measurements on NPOC extracts.

## DISCUSSION

### Method Evaluation

The method described here holds promise as a fast and simple procedure to extract and isolate NPOC from carbonate samples. Extensive testing has provided encouraging results, which provide a foundation for further development and refinement of the method. One of the key advantages of the method lies in the comparatively small sample sizes required. Depending on the amount of NPOC present in a stalagmite, as little as 50 mg sample mass are required for a high-precision IRMS  $\delta^{13}\text{C}$  measurement, and 100-200 mg for an AMS  $^{14}\text{C}$  measurement. This is similar to amounts reported by Blyth et al. (2013a, 2013b) for  $\delta^{13}\text{C}$ , and paves the way for conducting high-resolution studies of isotopic variations in NPOC from stalagmites. Additionally, the simple procedure, conducted entirely in one single vial, greatly reduces the risk of contamination by laboratory procedures, considered a major problem for studies of organic matter in stalagmites (Wynn and Brocks, 2014). Indeed, the contamination on single runs with this method can be as low as  $0.4 \pm 0.1 \mu\text{g C}$  ( $F^{14}\text{C} 0.15 \pm 0.04$ ), which greatly improves confidence in the interpretation of NPOC  $\delta^{13}\text{C}$  and  $^{14}\text{C}$  signatures even on very small samples ( $<10 \mu\text{g C}$ ). Due to blank fluctuations, we recommend running a complete standard curve,

ideally with 5 or more standards for both end members, with each sample run. Moreover, it appears that the sucrose standard is very susceptible to degradation once in solution, and future tests should investigate the use of a different modern standard with similar specifications (e.g., oxalic acid). Lowest blank contributions are typically obtained using freshly prepared standard solutions and oxidant (re-precipitated using ultra-pure water). The chemical pre-treatment standards tend to have slightly lower  $F^{14}C$  compared to the WCO standards (but the difference is not significant), which could point towards a minor blank contribution from the  $H_3PO_4$ . Although previous studies did not report blank issues related to the acid used (Lang et al., 2016, 2013, 2012), future studies should investigate how the much larger volume of acid needed for this method might influence overall blank contributions (e.g., Blyth et al., 2006). Storage times of up to three weeks do not result in increased blank contribution, e.g., from rubber septa degradation. However, we still recommend swift analysis of prepared extracts, ideally within days of the oxidation (but allowing enough time for solution re-equilibration after sample heating, i.e., ~24 hours), to achieve best results. Finally, prolonged storage of powdered carbonate samples should be avoided, as sorption of extraneous carbon on carbonate is common (Stipp and Hochella, 1991). Both stalagmites YOK-I and YOK-G were sampled shortly (hours – days) before analysis, and therefore we do not expect sorption effects to play a major role. Confidence in the results presented here stem from (i) steadily increasing NPOC concentrations with increasing sample size, suggesting that the carbon extracted is likely inherent to the sample, and not introduced by external background contamination, and (ii) NPOC  $\delta^{13}C$  values that are consistent with organic biomass, most likely reflecting carbon sources from terrestrial vegetation or microbial activity. However, our results show significant variability, both within replicate NPOC samples, as well as in the relationship between NPOC and  $CaCO_3$  values. This is likely the result of variable matrix effects as a function of sample type, as well in some cases incomplete decarbonation. We discuss these issues further below.

### Decarbonation Efficiency

Ensuring the complete removal of inorganic carbon proved to be the most difficult step of the method development. Subjecting the samples to a weak vacuum or to sonication was often successful in removing all  $CaCO_3$  from the solution, but the efficacy of the method still has reproducibility issues, especially for some stalagmites (e.g., TSAL). Decarbonation using rotary evaporation was the only method that reliably removed all  $CaCO_3$  from solution in all tested stalagmites, but in our case introduced large blanks, probably from the oil pumps (Suppl. fig. 1). However, this should not discourage others to test the use of a rotary evaporator, as this is the standard technique for DOC analysis of aquatic samples, and can often be employed successfully (Bryan et al., 2017). The other methods tested (desiccator and sonication) have the advantage of allowing a much higher throughput of sample batches compared to the rotary

**Commented [SSE3]:** Okay, but didn't some of your previous results suggest that this isn't much of an issue in reality?

evaporator, an essential quality if the method is to be applied to high-resolution studies. In this study, reproducibility and decarbonation efficiency were assessed by analysing chemical pretreatment standards and carbonate samples without oxidant. This approach, albeit time and resource consuming, allows to assess contamination and decarbonation individually, ideally for each run, and is advantageous for cases where method reproducibility is problematic.

Quantification of the amount of inorganic carbon in the NPOC extracts remains difficult, because the amount and isotope value of the organic 'end member' is not known. A simple isotopic mass balance can be carried out:

$$A_m \times \delta^{13}C_m = X \times \delta^{13}C_{ic} + (A_m - X) \times \delta^{13}C_{oc} \quad (1)$$

where  $A_m$  and  $\delta^{13}C_m$  are the measured amount and  $\delta^{13}C$  of carbon in the samples,  $\delta^{13}C_{ic}$  is the  $\delta^{13}C$  of the inorganic carbon,  $\delta^{13}C_{oc}$  is the  $\delta^{13}C$  value of the organic end member.  $X$  is the amount of inorganic carbon. We assume that the OC is entirely derived from C3-plants, a good approximation for all the caves studied here, resulting in an organic end member  $\delta^{13}C$  value of -25‰ VPDB. For stalagmite YOK-K, which shows the most consistent  $\delta^{13}C$  values for NPOC (Fig. 5B), mass balance reveals that about 1.2 - 4 µg C are likely  $CaCO_3$ -derived, which amounts to 2-11% of the original  $CaCO_3$  remaining in the solution. For the other stalagmites, the scatter between different measurements is much larger, and it is not straightforward to calculate the amount of  $CaCO_3$  remaining in the solution. This shows that complete removal of residual inorganic carbon from the samples remains a challenge, with implications for the fidelity of isotopic values measured in NPOC. Residual carbonate can also be detected in the IAEA-C1 vials spiked with phthalic acid (Suppl. Fig. 2), where larger samples display lower  $F^{14}C$  and less negative  $\delta^{13}C$  values, suggesting incomplete decarbonation. This was confirmed by tests using the IAEA-C2 standard ( $F^{14}C = 0.41$ ,  $\delta^{13}C = -8.25$ ‰ VPDB, not shown).

Combined  $\delta^{13}C$  and  $^{14}C$  datasets can help distinguish and exclude compromised samples. For example, samples from YOK-I batch A (YOK-I A, analysed in May 2016) have markedly lower  $F^{14}C$  and less negative  $\delta^{13}C$  values compared to both a previous analysis and to the samples of YOK-G (Fig. 7). These results suggest that the YOK-I A samples are affected by incomplete decarbonation, and thus should be excluded from further interpretation. Similarly, TSAL proved to be an especially difficult stalagmite to achieve complete decarbonation, which might point towards an inherent matrix effect that is more pronounced in this stalagmite than in others (Suppl. Fig. 3). More detailed studies of mineralogy and microstructure (e.g., through X-ray diffraction or scanning electron microscopy) in the samples should be encouraged in future studies, to better characterise the sample matrix.

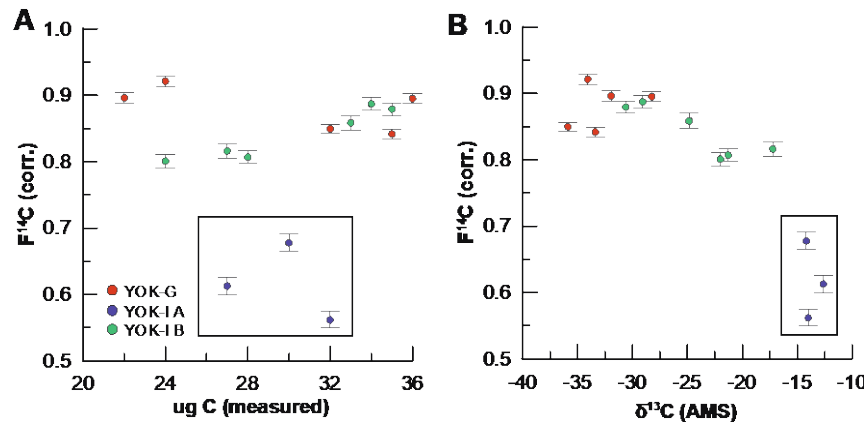


**Fig. 7.:** Comparison of the results for stalagmites YOK-I and YOK-G. Samples from YOK-I analysed during May 2016 (YOK-I A), likely affected by incomplete decarbonation, are highlighted by the black box.

#### Significance for interpretation of NPOC in stalagmites

The pronounced bomb spikes found in the carbonate of stalagmites YOK-I and YOK-G (Fig. 6) suggests that the majority of carbon transferred to the cave is cycled rapidly, and no large reservoir of pre-aged carbon is present. Previously published results on  $^{14}C$  analysis of water extractable organic carbon (WEOC) from soil samples collected above the Yok Balum Cave reflect the dominant contribution of very young OC from the soil, with 96% of the soil carbon being less than 50 years old (Lechleitner et al., 2016b). This is likely a function of the shallow thickness of the host rock above the cave ( $\sim 14\ m$ ), and the rapid response of the active drips to increases in rainfall (peaks during large rainfall events, and a general increase in drip rate over the rainy season; Ridley et al., 2015), which lead to rapid surface to cave signal transfer and minimise input from deeper carbon sources within the host rock. Compared to the test stalagmites from mid-latitude sites (BB2 and TSAL), the Yok Balum Cave stalagmites have higher concentrations of NPOC, which might additionally point towards a faster carbon transfer at this tropical location (Fig. 5A).

The NPOC  $F^{14}C$  from stalagmites YOK-I and YOK-G shows good agreement with the progression of the bomb spike rise in the carbonate of both stalagmites (Fig. 6). Compared to the carbonate  $F^{14}C$  however, the NPOC signal is dampened and overall  $F^{14}C$  is much lower. This is somewhat counterintuitive, as one would expect the carbonate, affected by  $^{14}C$ -dead host rock carbon, to be more depleted with respect to the vegetation-derived NPOC  $F^{14}C$ . At this stage, methodological issues, such as an unaccounted contamination source or stripping of more volatile molecules during purging (Lang et al., 2016, 2010) cannot be entirely ruled out. However, our extensive blank assessment, and the fact that the chemical pre-treatment

standards are not significantly different from the WCO standards, suggest that our results are robust, and the signal is likely real. One way to explain the difference between NPOC and carbonate  $^{14}\text{C}$  signatures in stalagmites YOK-I and YOK-G is through a contribution of OC from a refractory (insoluble and non-hydrolysable) pool that is not sourced from the soil. This could be related to a deep carbon source in the karst, as previously recognised in other karst systems (Benavente et al., 2010; Bergel et al., 2017; Matthey et al., 2016; Noronha et al., 2015). Although these studies focused on the presence of elevated  $p\text{CO}_2$  deeper in the karst that contribute carbon depleted in  $^{14}\text{C}$  to the drip water solution, it is also possible that refractory organic compounds are transported to the cave from such a source. Similarly, organic matter produced *in situ* (on the cave walls or on the stalagmites themselves) by microbial communities has been suggested as an important source of OC in stalagmites (Blyth et al., 2014; Lechleitner et al., 2017; Tisato et al., 2015), and could be responsible for the divergence between inorganic and organic carbon in stalagmites. A third potential source of refractory carbon in the karst system is fossil OC leached from the bedrock carbonate rock itself, e.g., through partial microbial oxidation. Such ‘petrogenic OC’ can have a measurable impact on bulk  $\text{F}^{14}\text{C}$  values, e.g., in rivers (Bouchez et al., 2010; Galy et al., 2008; Hemingway et al., 2018), and has been identified as an important component of speleothem OC before (Gázquez et al., 2012). One challenge to these explanations is the inverse trend found in stalagmite YOK-K, where the carbonate  $^{14}\text{C}$  is older than the NPOC, which might point towards contamination from a modern OC source during sampling, given that this is the sample with the highest NPOC concentrations tested here.

At present, our dataset does not allow a more definitive attribution of a single process (or a combination of several processes) that can explain the contrasting behaviour of inorganic and organic carbon in the stalagmites. It should be noted, however, that a previous study seeking to characterise the molecular spectrum of the dissolved organic matter (DOM) at Yok Balum Cave found very different molecular composition of soil and drip waters, and stalagmites, with the stalagmite DOM fingerprint suggesting a contribution from microbial organic matter (Lechleitner et al., 2017). Irrespective of these unresolved issues, it is clear that at Yok Balum Cave, OC entrapped within stalagmites derives from one or several dynamic pool(s). Whether stalagmites from other locations (e.g., high latitudes) exhibit similar characteristics, both in the magnitude and cycling of organic matter, remains to be seen.

## CONCLUSIONS

We present first results from a method development study on extraction and isotopic ( $\delta^{13}\text{C}$  and  $^{14}\text{C}$ ) characterisation of speleothem NPOC. The advantages of the method lie in its simple, rapid protocol that is carried out in a single vial, minimising the potential for contamination through laboratory procedures, and in the small sample sizes needed. Encouraging results indicate that

the extracted carbon is likely inherent to the sample and organic, as shown by depleted  $\delta^{13}\text{C}$  values. However, unresolved issues remain, and need to be addressed by future studies to fully make use of the method. A major remaining issue is incomplete sample decarbonation, resulting in biased isotope values. Although anomalous samples can be detected via combined  $\delta^{13}\text{C}$  and  $^{14}\text{C}$  analyses, further methodological improvements are needed before the method can be made routine. Complete decarbonation was so far achieved only when subjecting the samples to a weak vacuum using a rotary evaporator. Unfortunately, this method had to be abandoned as it resulted in contamination of the samples from the oil pump. Sonication appears to be a promising tool to increase decarbonation efficiency, with the advantage of working on a closed vial and thus minimising contamination, but needs to be tested more thoroughly. Sample contamination through laboratory procedures need to be minimised, as this method is very susceptible to blank effects. Ideally, a designated “clean” fume hood should be used for this method only, and in any case work producing large amounts of dust should not be carried out in the same room as the wet oxidation procedure. The sucrose standard appears to be very susceptible to alteration, and might be better replaced by another compound with modern  $\text{F}^{14}\text{C}$  and similar  $\delta^{13}\text{C}$  (e.g., oxalic acid). Subsequent studies that further improve upon methodologies and expand measurements to a broader suite of stalagmites and their host cave systems should add important new constraints on carbon cycle processes in karst systems and organic signals preserved in stalagmites. Moreover, detailed investigations on organic and inorganic carbon fluxes in karst systems and the isotopic fingerprint of processes acting on them could provide important insights into the local carbon cycle and the sources of carbon in speleothems.

#### ACKNOWLEDGEMENT

We thank the staff at LIP, especially Lukas Wacker, and Daniel Montluçon, Stewart Bishop and Madalina Jaggi at the Geological Institute, ETH Zurich for their assistance with sample analysis. We thank José Mes for assistance during fieldwork at Yok Balum Cave. We gratefully acknowledge Sebastian Breitenbach, Denis Scholz, and Birgit Plessen for provision of sample materials from stalagmites BB2 and TSAL. We thank Andy Baker and Kathleen Johnson for critical reviewing of this manuscript, and the editorial team at *Radiocarbon*. This research was supported by the European Research Council grant 240167 grant to JULB, and by Swiss National Science Foundation grant P2EZP2\_172213 to FAL. Field collection was supported additionally by the National Science Foundation (grant HSD 0827305) and the Alphawood Foundation.

#### REFERENCES

Baker, A., Genty, D., 1999. Fluorescence wavelength and intensity variations of cave waters.



474 J. Hydrol. 217, 19–34. doi:10.1016/S0022-1694(99)00010-4

475 Benavente, J., Vadillo, I., Carrasco, F., Soler, A., Liñán, C., Moral, F., 2010. Air Carbon  
476 Dioxide Contents in the Vadose Zone of a Mediterranean Karst. *Vadose Zo. J.* 9, 126–  
477 136. doi:10.2136/vzj2009.0027

478 Bergel, S.J., Carlson, P.E., Larson, T.E., Wood, C.T., Johnson, K.R., Banner, J.L., Breecker,  
479 D.O., 2017. Constraining the subsoil carbon source to cave-air CO<sub>2</sub> and speleothem  
480 calcite in central Texas. *Geochim. Cosmochim. Acta* 217, 112–127.  
481 doi:10.1016/j.gca.2017.08.017

482 Birdwell, J.E., Engel, A.S., 2010. Characterization of dissolved organic matter in cave and  
483 spring waters using UV-Vis absorbance and fluorescence spectroscopy. *Org. Geochem.*  
484 41, 270–280. doi:10.1016/j.orggeochem.2009.11.002

485 Blyth, A.J., Baker, A., Collins, M.J., Penkman, K.E.H., Gilmour, M.A., Moss, J.S., Genty, D.,  
486 Drysdale, R.N., 2008. Molecular organic matter in speleothems and its potential as an  
487 environmental proxy. *Quat. Sci. Rev.* 27, 905–921. doi:10.1016/j.quascirev.2008.02.002

488 Blyth, A.J., Farrimond, P., Jones, M., 2006. An optimised method for the extraction and  
489 analysis of lipid biomarkers from stalagmites. *Org. Geochem.* 37, 882–890.  
490 doi:10.1016/j.orggeochem.2006.05.003

491 Blyth, A.J., Hartland, A., Baker, A., 2016. Organic proxies in speleothems - New  
492 developments, advantages and limitations. *Quat. Sci. Rev.* 149, 1–17.  
493 doi:10.1016/j.quascirev.2016.07.001

494 Blyth, A.J., Hua, Q., Smith, A., Frisia, S., Borsato, A., Hellstrom, J., 2017. Exploring the  
495 dating of “dirty” speleothems and cave sinters using radiocarbon dating of preserved  
496 organic matter. *Quat. Geochronol.* 39, 92–98. doi:10.1016/j.quageo.2017.02.002

497 Blyth, A.J., Jex, C.N., Baker, A., Khan, S.J., Schouten, S., 2014. Contrasting distributions of  
498 glycerol dialkyl glycerol tetraethers (GDGTs) in speleothems and associated soils. *Org.*  
499 *Geochem.* 69, 1–10. doi:10.1016/j.orggeochem.2014.01.013

500 Blyth, A.J., Shutova, Y., Smith, C., 2013a.  $\delta^{13}\text{C}$  analysis of bulk organic matter in  
501 speleothems using liquid chromatography-isotope ratio mass spectrometry. *Org.*  
502 *Geochem.* 55, 22–25. doi:10.1016/j.orggeochem.2012.11.003

503 Blyth, A.J., Smith, C.I., Drysdale, R.N., 2013b. A new perspective on the  $\delta^{13}\text{C}$  signal  
504 preserved in speleothems using LC-IRMS analysis of bulk organic matter and  
505 compound specific stable isotope analysis. *Quat. Sci. Rev.* 75, 143–149.  
506 doi:10.1016/j.quascirev.2013.06.017

507 Borsato, A., Frisia, S., Jones, B., van der Borg, K., 2000. Calcite moonmilk: crystal  
508 morphology and environment of formation in caves in the Italian Alps. *J. Sediment. Res.*  
509 70, 1170–1190.

510 Bosle, J.M., Mischel, S.A., Schulze, A.-L., Scholz, D., Hoffmann, T., 2014. Quantification of

low molecular weight fatty acids in cave drip water and speleothems using HPLC-ESI-IT / MS — development and validation of a selective method. *Anal. Bioanal. Chem.* 406, 3167–3177. doi:10.1007/s00216-014-7743-6

Bouchez, J., Beyssac, O., Galy, V., Gaillardet, J., France-Lanord, C., Maurice, L., Moreira-Turcq, P., 2010. Oxidation of petrogenic organic carbon in the Amazon floodplain as a source of atmospheric CO<sub>2</sub>. *Geology* 38, 255–258. doi:10.1130/G30608.1

Bryan, E., Meredith, K.T., Baker, A., Andersen, M.S., Post, V.E.A., 2017. Carbon dynamics in a Late Quaternary-age coastal limestone aquifer system undergoing saltwater intrusion. *Sci. Total Environ.* 607–608, 771–785. doi:10.1016/j.scitotenv.2017.06.094

Einsiedl, F., Hertkorn, N., Wolf, M., Frommberger, M., Schmitt-Kopplin, P., Koch, B.P., 2007. Rapid biotic molecular transformation of fulvic acids in a karst aquifer. *Geochim. Cosmochim. Acta* 71, 5474–5482. doi:10.1016/j.gca.2007.09.024

Fahrni, S.M., Wacker, L., Synal, H.A., Szidat, S., 2013. Improving a gas ion source for 14C AMS. *Nucl. Instruments Methods Phys. Res. Sect. B* 294, 320–327. doi:10.1016/j.nimb.2012.03.037

Galy, V., Beyssac, O., France-Lanord, C., Eglinton, T., 2008. Recycling of graphite during Himalayan erosion: A geological stabilization of carbon in the crust. *Science* (80-. ). 322, 943–945. doi:10.1126/science.1161408

Gázquez, F., Calaforra, J.M., Rull, F., Forti, P., García-Casco, A., 2012. Organic matter of fossil origin in the amberine speleothems from El Soplao Cave (Cantabria, Northern Spain). *Int. J. Speleol.* 41, 113–123. doi:10.5038/1827-806X.41.1.12

Genty, D., Konik, S., Valladas, H., Blamart, D., Hellstrom, J., Touma, M., Moreau, C., Dumoulin, J.-P., Nouet, J., Dauphin, Y., Weil, R., 2011. Dating the lascaux cave gourd formation. *Radiocarbon* 53, 479–500.

Haghipour, N., Ausin, B., Usman, M., Ishikawa, N.F., Wacker, L., Welte, C., Ueda, K., Eglinton, T.I., 2018. Compound-Specific Radiocarbon Analysis (CSRA) by Elemental Analyzer- Accelerator Mass Spectrometry (EA-AMS): Precision and Limitations. *Anal. Chem.* doi:10.1021/acs.analchem.8b04491

Hanke, U.M., Wacker, L., Haghipour, N., Schmidt, M.W.I., Eglinton, T.I., McIntyre, C.P., 2017. Comprehensive radiocarbon analysis of benzene polycarboxylic acids (BPCAs) derived from pyrogenic carbon in environmental samples. *Radiocarbon* 59, 1103–1116. doi:10.1017/RDC.2017.44

Heidke, I., Scholz, D., Hoffmann, T., 2018. Quantification of lignin oxidation products as vegetation biomarkers in speleothems and cave drip water. *Biogeosciences* 15, 5831–5845. doi:10.5194/bg-2018-253

Hemingway, J.D., Hilton, R.G., Hovius, N., Eglinton, T.I., Haghipour, N., Wacker, L., Chen, M., Galy, V. V., 2018. Microbial oxidation of lithospheric organic carbon in rapidly

eroding tropical mountain soils. *Science* (80-. ). 360, 209–212.  
doi:10.1126/science.aao6463

Lang, S.Q., Bernasconi, S.M., Fröh-Green, G.L., 2012. Stable isotope analysis of organic carbon in small ( $\mu\text{g C}$ ) samples and dissolved organic matter using a GasBench preparation device. *Rapid Commun. Mass Spectrom.* 26, 9–16. doi:10.1002/rcm.5287

Lang, S.Q., Butterfield, D.A., Schulte, M., Kelley, D.S., Lilley, M.D., 2010. Elevated concentrations of formate, acetate and dissolved organic carbon found at the Lost City hydrothermal field. *Geochim. Cosmochim. Acta* 74, 941–952.  
doi:10.1016/j.gca.2009.10.045

Lang, S.Q., Fröh-Green, G.L., Bernasconi, S.M., Wacker, L., 2013. Isotopic ( $\text{d}^{13}\text{C}$ ,  $\text{D}^{14}\text{C}$ ) analysis of organic acids in marine samples using wet chemical oxidation. *Limnol. Oceanogr. Methods* 11, 161–175. doi:10.4319/lom.2013.11.161

Lang, S.Q., McIntyre, C.P., Bernasconi, S.M., Fröh-Green, G.L., Voss, B.M., Eglinton, T.I., Wacker, L., 2016. Rapid  $^{14}\text{C}$  Analysis of Dissolved Organic Carbon in Non-Saline Waters. *Radiocarbon* 58, 505–515. doi:10.1017/RDC.2016.17

Lechleitner, F.A., Baldini, J.U.L., Breitenbach, S.F.M., Fohlmeister, J., McIntyre, C., Goswami, B., Jamieson, R.A., van der Voort, T.S., Prufer, K., Marwan, N., Culleton, B.J., Kennett, D.J., Asmerom, Y., Polyak, V., Eglinton, T.I., 2016a. Hydrological and climatological influences on a very high resolution tropical stalagmite radiocarbon record. *Geochim. Cosmochim. Acta*. doi:http://dx.doi.org/10.1016/j.gca.2016.08.039

Lechleitner, F.A., Baldini, J.U.L., Breitenbach, S.F.M., Fohlmeister, J., McIntyre, C., Goswami, B., Jamieson, R.A., van der Voort, T.S., Prufer, K., Marwan, N., Culleton, B.J., Kennett, D.J., Asmerom, Y., Polyak, V., Eglinton, T.I., 2016b. Hydrological and climatological controls on radiocarbon concentrations in a tropical stalagmite. *Geochim. Cosmochim. Acta* 194, 233–252. doi:10.1016/j.gca.2016.08.039

Lechleitner, F.A., Dittmar, T., Baldini, J.U.L., Prufer, K.M., Eglinton, T.I., 2017. Molecular signatures of dissolved organic matter in a tropical karst system. *Org. Geochem.* 113. doi:10.1016/j.orggeochem.2017.07.015

Li, X., Hu, C., Huang, J., Xie, S., Baker, A., 2014. A 9000-year carbon isotopic record of acid-soluble organic matter in a stalagmite from Heshang Cave, central China: Paleoclimate implications. *Chem. Geol.* 388, 71–77.  
doi:10.1016/j.chemgeo.2014.08.029

Mattey, D.P., Atkinson, T.C., Barker, J.A., Fisher, R., Latin, J.-P., Durell, R., Ainsworth, M., 2016. Carbon dioxide, ground air and carbon cycling in Gibraltar karst. *Geochim. Cosmochim. Acta* 184, 88–113. doi:10.1016/j.gca.2016.01.041

Noronha, A.L., Johnson, K.R., Southon, J.R., Hu, C.C., Ruan, J., McCabe-Glynn, S., 2015. Radiocarbon evidence for decomposition of aged organic matter in the vadose zone as

the main source of speleothem carbon. *Quat. Sci. Rev.* 127, 37–47.  
doi:10.1016/j.quascirev.2015.05.021

Perrette, Y., Poulénard, J., Protière, M., Fanget, B., Lombard, C., Miège, C., Quiers, M.,  
Nafferchoux, E., Pépin-Donat, B., 2015. Determining soil sources by organic matter  
EPR fingerprints in two modern speleothems. *Org. Geochem.* 88, 59–68.  
doi:10.1016/j.orggeochem.2015.08.005

Quiers, M., Perrette, Y., Chalmin, E., Fanget, B., Poulénard, J., 2015. Geochemical mapping  
of organic carbon in stalagmites using liquid-phase and solid-phase fluorescence. *Chem.*  
*Geol.* 411, 240–247. doi:10.1016/j.chemgeo.2015.07.012

Reimer, P.J., Brown, T.A., Reimer, R.W., 2004. Discussion: reporting and calibration of post-  
bomb  $^{14}\text{C}$  data. *Radiocarbon* 46, 1299–1304.

Ridley, H.E., Asmerom, Y., Baldini, J.U.L., Breitenbach, S.F.M., Aquino, V. V., Prufer,  
K.M., Culleton, B.J., Polyak, V., Lechleitner, F.A., Kennett, D.J., Zhang, M., Marwan,  
N., Macpherson, C.G., Baldini, L.M., Xiao, T., Peterkin, J.L., Awe, J., Haug, G.H.,  
2015. Aerosol forcing of the position of the intertropical convergence zone since ad  
1550. *Nat. Geosci.* 8, 195–200. doi:10.1038/ngeo2353

Ruff, M., Wacker, L., Gägeler, H.W., Suter, M., Synal, H.-A., Szidat, S., 2007. A gas ion  
source for radiocarbon measurements at 200 kV. *Radiocarbon* 49, 307–314.

Shabarova, T., Villiger, J., Morenkov, O., Niggemann, J., Dittmar, T., Pernthaler, J., 2014.  
Bacterial community structure and dissolved organic matter in repeatedly flooded  
subsurface karst water pools. *Microbiol. Ecol.* 89, 111–126. doi:10.1111/1574-  
6941.12339

Stipp, S.L., Hochella, M.F.J., 1991. Structure and bonding environments at the calcite surface  
as observed with X-ray photoelectron spectroscopy (XPS) and low energy electron  
diffraction (LEED). *Geochim. Cosmochim. Acta* 55, 1723–1736.

Tisato, N., Torriani, S.F.F., Monteux, S., Sauro, F., De Waele, J., Tavagna, M.L., D’Angeli,  
I.M., Chailloux, D., Renda, M., Eglinton, T.I., Bontognali, T.R.R., 2015. Microbial  
mediation of complex subterranean mineral structures. *Sci. Rep.* 5, 15525.  
doi:10.1038/srep15525

Vogel, J.C., 1980. Fractionation of the Carbon Isotopes During Photosynthesis, in:  
*Sitzungsberichte Der Heidelberger Akademie Der Wissenschaften*. pp. 111–135.

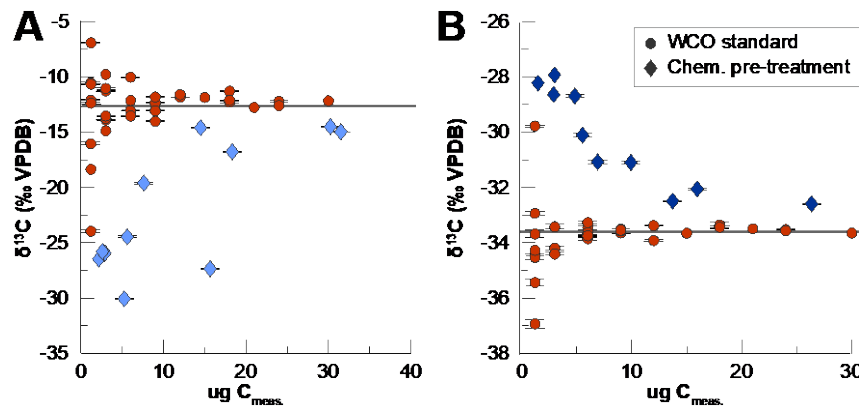
Wacker, L., Christl, M., Synal, H.A., 2010. Bats: A new tool for AMS data reduction. *Nucl.*  
*Instruments Methods Phys. Res. Sect. B* 268, 976–979. doi:10.1016/j.nimb.2009.10.078

Wynn, P.M., Brocks, J.J., 2014. A framework for the extraction and interpretation of organic  
molecules in speleothem carbonate. *Rapid Commun. Mass Spectrom.* 28, 845–854.  
doi:10.1002/rcm.6843

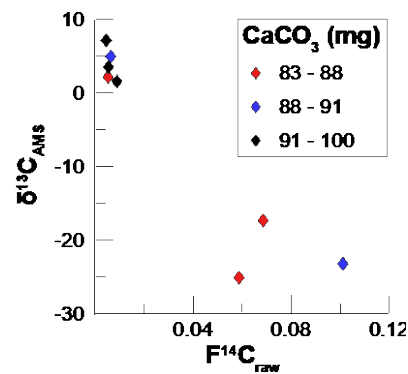
**Supplementary materials:**

**Supplementary Table 1:** Summary of all standards processed during this study, with their blank correction according to Hanke et al. (2017) and Haghipour et al., (*in review*).

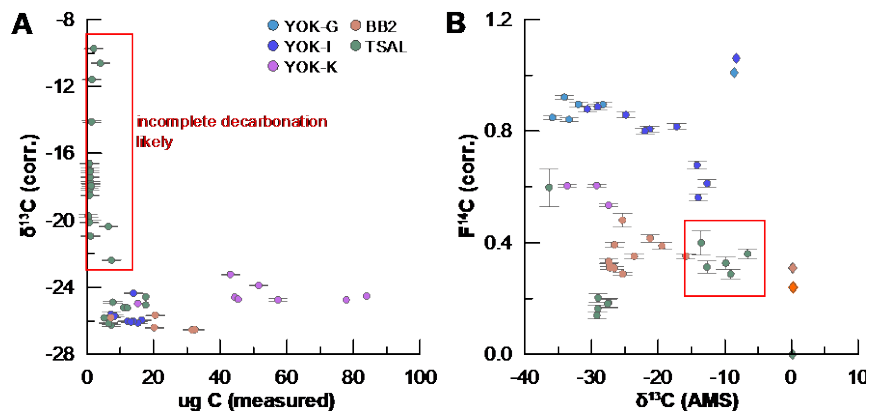
**Supplementary Table 2:** All results on  $^{14}\text{C}$  measurements on stalagmite WCO extracts.



**Supplementary Fig 1.:** Comparison between standard and pre-treatment standards after rotary evaporation treatment, showing large offsets from the real value. Chemical pre-treatment standards that were analysed for  $\delta^{13}\text{C}$  show large offsets compared to the standards (A – sucrose, B – phthalic acid) due to extraneous carbon introduced by the rotary evaporator.



**Supplementary Fig 2.:** Results for vials containing a known amount of IAEA C1 carbonate ( $^{14}\text{C}$ -dead), spiked with phthalic acid. A weak relationship between sample size and isotopic signature of the WCO is visible, with larger samples showing lower  $F^{14}\text{C}$  and less negative  $\delta^{13}\text{C}$  values, suggesting incomplete decarbonation.



**Supplementary Fig 3.:** Matrix effects resulting in frequent incomplete decarbonation in stalagmite TSAL.